ISBN: 978-3-95450-240-0 ISSN: 2673-5547 doi:10.18429/JACoW-HIAT2022-TUP19

FIRST TESTS OF MODEL-BASED LINAC PHASING IN ISAC-II

S. Kiy*, R. Baartman, O. Kester, O. Shelbaya
TRIUMF, Vancouver, BC, Canada

Abstract

As the e-linac and ARIEL facilities at TRIUMF progress, the impending complexity of operating three simultaneous rare ion beams (RIBs) approaches. To help prepare for this, a framework for the development of High Level Applications has been constucted, upon which multiple avenues for improvement towards model-based and automated tuning are being pursued. Along one of these avenues, the 40-cavity superconducting ISAC-II heavy ion linac has been studied and modelled in the envelope code transoptr. This has allowed for real-time integration through the on-axis fields, fitting focal strengths of solenoids to achieve desired beam waists, and calculation of necessary cavity phases to achieve a desired output energy for given input beam parameters. Initial tests have been completed, successfully phasing up to 37 cavities using the transoptr model and achieving a final output energy within 1% of the expected while maintaining nominal (>90%) transmission. A summary of the calibration of the model to the machine is given, followed by results of the phasing tests and an outlook towards future improvements.

INTRODUCTION

The Isotope Separator and ACcelerator (ISAC) facility at TRIUMF serves a wide assortment of experiments that study nuclear structure, materials science, nuclear astrophysical reaction rates, and more. Stable beams from the Off-line Ion Source (OLIS) or radioactive ion beams from the target stations can be delieved to low, medium, or high energy sections depending on the amount of post-acceleration required. The ISAC-I medium energy section, completed in 2001 [1], provides ion beams from 0.15 to 1.8 MeV/u while the ISAC-II high energy section, completed in two phases in 2006 and 2010 [2], can deliver beams from 1.5 up to as high as 16.5 MeV/u.[1]

Acceleration in the ISAC-II linac is provided by forty superconducting two-gap quarter wave niobium cavities, operating at 4.2 K. Cavities are distributed over eight cryomodules, each containing one superconducting solenoid.

MOTIVATION

Typical experiments served by the ISAC-II linac run for approximately 7 days. Overhead for these experiments to adjust the accelerators for new beam properties is typically scheduled for 24 hours. The portion of this overhead required for the optimization of the ISAC-II linac is regularly over 8 hours and requires expert assistance or senior operators.

The optimization itself is a complex process, as it involves the user turning on one cavity at a time and scanning the phase to identify the desired setpoint. This is further complicated by the large energy gain relative to the incoming energy for the first few cryomodules, which impacts the transverse tune and requires re-optimization of solenoids and quadrupoles.

Basically, it is a problem of a large configuration space with interdependent tuning parameters:

- 40 cavities x 2 adjustable parameters (phase, amplitude)
- 8 solenoids x 1 adjustable parameter (current)
- 8 cryomodules x 2 adjustable parameters (x, y steerers)

This has motivated a more model-based approach to the operation of the ISAC-II superconducting linac.

HIGH LEVEL APPLICATIONS AT TRIUMF

The high-level applications (HLA) taskforce [3, 4] is tasked with using model-based tuning integrated with the control system to improve beam quality and reduce tuning overhead. This project is one of multiple such areas of study at TRIUMF and utilizes various components of the HLA framework, including python to EPICS communication, xml beamline information, and `TRANSOPTR` for beam envelope simulations.

MODEL CALIBRATION

Diagnostics

The time structure of the beam at three locations of known distance along the beamline are measured using flight time monitors (FTMs). Shown below in Fig.1, FTMs are an assembly consisting of a $50\mu m$ diameter biased tungsten wire that intersects the beam and emits secondary electrons.

These electrons are detected by a micro-channel plate (MCP) detector with a time resolution of < 100 ps, giving a resulting energy/nucleon resolution of under 0.1% [5]. The velocity or the ion beam is calculated as a weighted average using the arrival time at each of the possible 3 pairs of monitors [6].

With no time diagnostics within the linac itself, these three monitors located approximately 3, 5, and 14 metres downstream of the last accelerating cavity are the primary diagnostics used for both measuring the beam velocity and calibrating cavity phases in the model.

Phase Shifters

The fourty cavities in the ISAC-II linac are each driven independently, so each cavity has its own designated phase

* spencerkiy@triumf.ca
[1] 16.5 MeV/u is achievable here for A/q of 2.

ISBN: 978-3-95450-240-0 ISSN: 2673-5547 doi:10.18429/JACoW-HIAT2022-TUP19

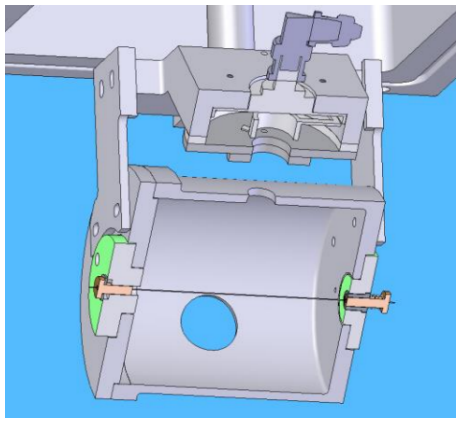

Figure 1: A model cutaway of one of the FTMs, showing the Tungsten wire as well as the beam port (bottom, centre of the picture) and the port for the MCP.

shifter to allow the user to adjust the cavity timing to the arrival of the beam. To allow for automated phasing, the exact behaviour of the phase shifter circuits was investigated. A vector voltmeter was used to measure the phase difference between the RF reference signal arriving at the phase shifter circuit to the output. This difference was recorded for varying setpoints of the phase shifter in the control system to measure the real phase change vs control system.

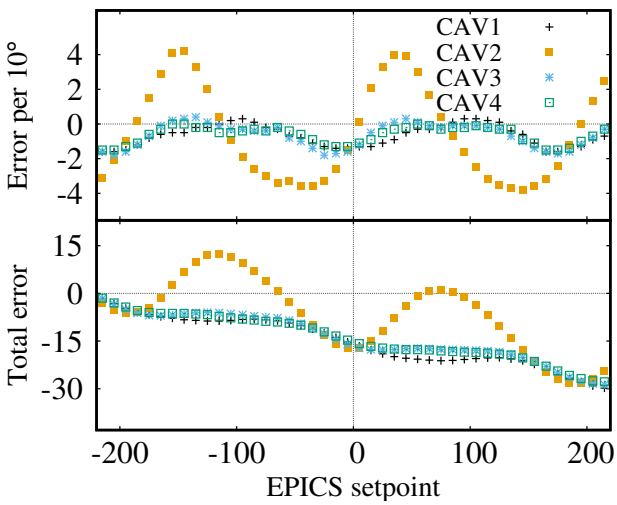

Figure 2: Measured error in phase per 10 degree step (above) and cumulative error from starting point of -220 degrees (below) vs setpoint in the control system.

As shown in Fig. 2, the relationship is non-linear and varies from one cavity to the next. To handle this, the phase behaviour was measured for all fourty cavities as well as three available global phase shifters, and input into a python package which converts between the control system setpoint and a phase in degrees prior to modelling.

The ISAC-II Linac Model in TRANSOPTR

TRANSOPTR is a first-order beam envelope code written in FORTRAN and developed at TRIUMF [7]. It calculates the beam's sigma matrix, representing the beam envelope in 6-dimensional phase space (x, P_x, y, P_y, z, P_z). Notable benefits include the available expertise at TRIUMF, fast execution times (on the order of 1 second), and the ability to integrate through an-axis field maps of accelerating cavities [8].

While model-based calculations of the necessary cavity phase could also use a drift-kick model and the transit-time factor approach - use of an envelope code like TRANSOPTR is advantageous as it also allows the desired optimization of transverse focusing elements.

For a given configuration of the linac, the cavity amplitudes from the control system are fed into the model, which can then model RF defocusing effects and run optimizations of solenoid strengths to achieve the desired beam waist at the desired location between each cryomodule.

TRANSOPTR takes as inputs the on-axis magnetic field (B_z) for the solenoids and the on-axis electric field ($\mathscr{E}_z$) for the superconducting RF cavities. The B_z field maps were measured by the vendor, Accel, in Germany for the superconducting solenoids while the $\mathscr{E}_z$ field maps, shown in Fig. 3 were simulated in CST microwave studios (V. Zyvagintsev, personal communication, November 11, 2021).

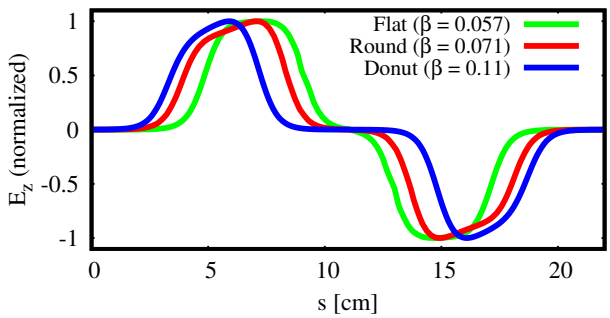

Figure 3: Normalized $\mathscr{E}_z$ field maps of the three cavity types found in the ISAC-II linac.

The evolution of the sigma matrix is governed by the envelope equation [8]

$$\sigma' = F \cdot \sigma + \sigma \cdot F^T \tag{1}$$

Where σ is the sigma (or covariance) matrix representing the beam in 6-dimensional phase space. The prime denotes a derivative with respect to s, the distance along design orbit. F is the infinitesimal transfer matrix, defined by:

$$X' = FX \tag{2}$$

Where X is the vector (x, P_x, y, P_y, z, P_z). The infinitesimal transfer matrix for an axially symmetric RF field [8] depends only on the longitudinal component of the on-axis electric field,

$$\mathscr{E}_z(s,t) = \mathscr{E}_z(s) \cdot cos(\omega t + \phi_i - \theta) \tag{3}$$

ISBN: 978-3-95450-240-0 ISSN: 2673-5547 doi:10.18429/JACoW-HIAT2022-TUP19

Where $\mathscr{E}_z$ is the longitudinal electric field map, ω is the RF angular frequency, ϕ is the control system phase, and θ is the cavity phase offset.

TRANSOPTR solves Eq. 1 by carrying out Runge-Kutte integration with an adaptive step size. The code also solves for the equations governing the total energy and time of flight.

BEAM-BASED CALIBRATION

Cavity Calibrations

The length of the RF lines for the fourty cavities differ, both from the master oscillator to the LLRF boards and amplifiers as well as from the amplifiers along the RF transmission lines to the cavities. To properly align the model with the machine, the phase offset of cavities, θ, must be established. The scaling between the control system amplitude and the peak electric field in the accelerating gaps must also be known.

To accomplish this, a calibration tune was established using a manual phasing method. Cavities are turned on one at at time and the control system phase is varied to a minimum of 5 different values, while using the FTM system to calculate the energy per nucleon at each of the phases. An optimization routine is then run to find the parameters θ and C that minimize the sum of the squared residuals as shown below in Eq. 4

$$S = \sum_{i=1}^{m} (E_i - f(\phi_i, C, \theta))^2 \tag{4}$$

Where

$$f(\phi_i, C, \theta) = W_{in} + \Delta E \tag{5}$$

Where W_{in} is the incoming energy of the beam. From Eq. 3, we have

$$\Delta E = q \int A \cdot C \cdot \mathscr{E}_{norm}(s) \cdot cos(\omega t + \phi_i - \theta) ds \tag{6}$$

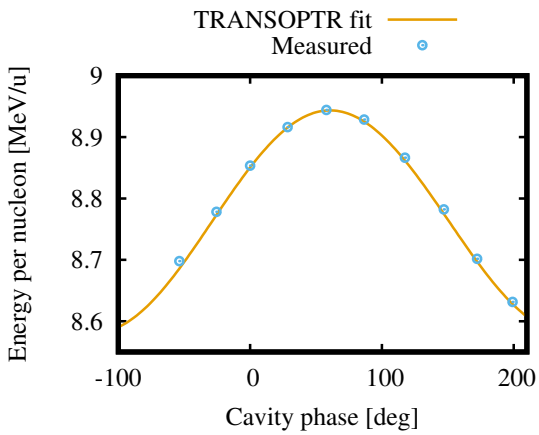

Figure 4: Energy vs cavity phase plot for one cavity, showing resulting fit between measured behaviour and the model.

Where q is the charge state of the beam, and the $\mathscr{E}_z$ field map has been broken down into the normalized field map shown in Fig. 3, the control system amplitude A, and the scaling parameter C. An example of a typical fit to the collected data is shown above in Fig. 4.

IMPLEMENTATION AND UI

Initial tests were carried out running the model from a terminal. Of course, a more robust and user-friendly interface will be required to transfer this automated phasing tool to operations.

To this end, a web-interface is being established using the HLA framework to provide operators with a UI. This phasing tool is being built in to an existing app which is a python process running within a Docker container. The app sends the long running optimization request to a backend process via celery, which the client's machine then polls periodically until the process is complete. An overview of the current operator interface is shown in Figures 5 and 6.

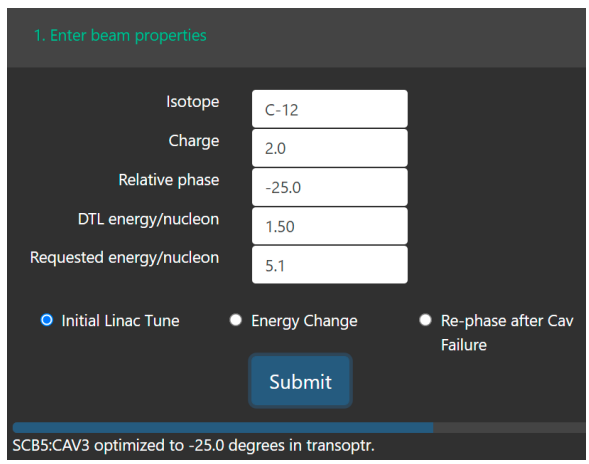

Figure 5: Web interface for operations to run the ISAC-II model for automatic calculation of cavity phases and solenoid strengths.

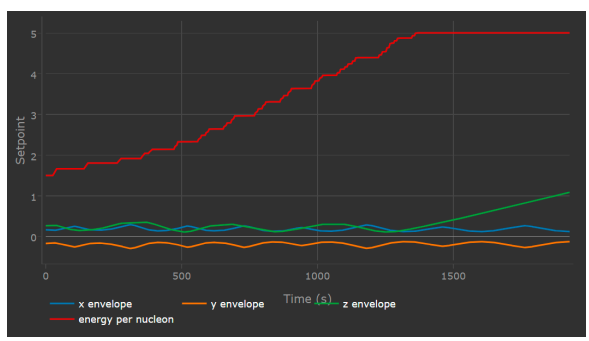

Figure 6: Envelope displayed on UI after model optimization.

ONLINE TESTS

A test was completed with 35 operational cavities, based on a single calibration tune at A/Q 4.5 from May of 2021.

ISBN: 978-3-95450-240-0 ISSN: 2673-5547 doi:10.18429/JACoW-HIAT2022-TUP19

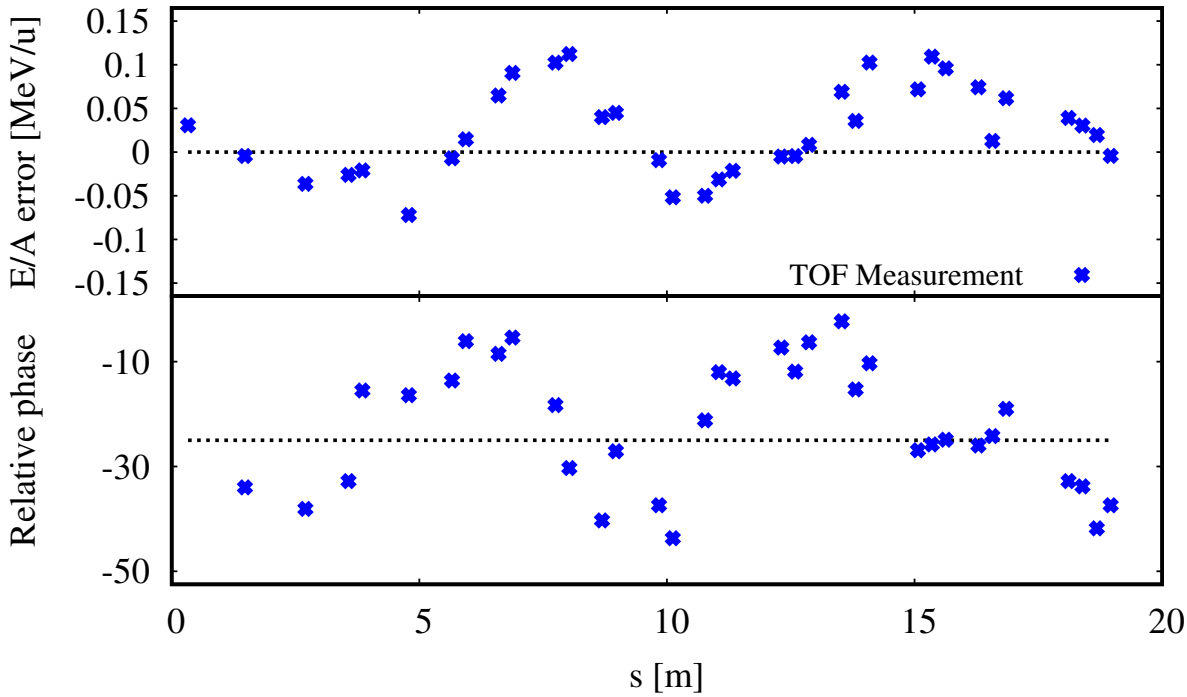

Figure 7: Measured energy and phase after each cavity of the test (blue) compared to expectations from the model (dashed line). X-axis is distance along the beamline.

The calibrated model was used to calculate the desired control system phase that gave a -25 degree relative phase and the expected energy output of each cavity.

To assess the accuracy of the model calculations, cavities were then turned on one at a time. Each cavity had its phase vs output energy behaviour measured (as done in calibration, shown in Fig. 4) and fit to quantify how far off the model was from the desired -25 degree relative phase. Finally, the cavity was set to the phase calculated by the model and transmission and energy were measured for further comparison to the model.

DISCUSSION

Shown above in Fig. 7, the energy per nucleon error in this test was less than 0.15 MeV/u while the cavity phase error was less than 20 degrees for all available cavities. Linac transmission averaged over 90% and the established tune was successfully used for delivery to an experiment.

The initial few cryomodules are suspected to be primary cause of error observed in Fig. 7. As demonstrated by the very first data point from the left on the top plot in Fig. 7, the energy error after the very first cavity is 0.03 MeV/u, which corresponds to an error of ~ 10% in the energy gained from this cavity. This could come solely from an error in the fit amplitude parameter C, from a phase error in the first cavity of ~ 4 degrees, or a combination of the two.

Due to the relatively low velocity through the first few cryomodules, this size of an energy error can produce a significant phase error at the next cavity - in this test the next operational cavity was 1.15 metres downstream, meaning the 0.03 MeV/u introduces a 20 degree phase error at the next cavity. Even if the rest of the cavities are set precisely correct, the mean energy and phase of the beam will now oscillate aroud the synchonus particle, similar to the behaviour seen in Fig. 7. For contrast, a 0.03 MeV/u energy error at 8.0 MeV/u over 1.15 m would only cause an error of 2 degrees at the next cavity.

Further work is planned to more carefully calibrate the early cavities in the linac, including a full 360 degree scan of the energy-phase output of the cavities at smaller step sizes. This can be difficult, as the relatively large energy gains of the first linac cavities have a significant impact on the transverse optics which require re-optimization to transport beam the ~ $32m$ downstream to reach all three FTMs. However, this initial model-based phasing approach will now expedite this process, enabling continuous improvment of the model and linac operation.

CONCLUSION

The ISAC-II linac has been modelled in TRANSOPTR and various calibration necessary for the model have been investigated. Tests of automated phasing have been carried out and have demonstrated the capability to now setup the linac for a new experiment in under an hour where it historically has required over 1 shift (8 hours).

REFERENCES

[1] R. E. Laxdal *et al.*, "Beam Commissioning and First Operation of the ISAC DTL at TRIUMF", in *Proc. 19th Particle Accel-*

ISBN: 978-3-95450-240-0 ISSN: 2673-5547 doi:10.18429/JACoW-HIAT2022-TUP19

erator Conf. (PAC'01), Chicago, IL, USA, Jun. 2001, paper FPAH112, pp. 3942–3944.

[2] M. Marchetto *et al.*, "The ISAC-II Linac Performance", in *Proc. 13th Int. Conf. on Heavy Ion Accelerator Technology (HIAT'15)*, Yokohama, Japan, Sep. 2015, paper WEM2I01, pp. 175–179.

[3] C. B. Barquest *et al.*, "Web-Based Control Room Applications at TRIUMF", in *Proc. 9th Int. Particle Accelerator Conf. (IPAC'18)*, Vancouver, Canada, Apr.-May 2018, pp. 4832–4835. doi:10.18429/JACoW-IPAC2018-THPML078

[4] S. Kiy *et al.*, "Beam Tuning Automation Activities at TRIUMF," presented at the 15th Heavy Ion Accelerator Technology Conf. (HIAT'22), Darmstadt, Germany, June 2022, paper TU2C4, this conference.

[5] V.A. Verzilov, R.E. Laxdal, M. Marchetto, and W.R. Rawnsley, "Time Domain Diagnostics for the ISAC-II Superconducting Heavy Ion Linac", in *Proc. 8th European Workshop on Beam Diagnostics and Instrumentation for Particle Accelerators (DIPAC'07)*, Venice, Italy, May 2007, paper WEPB07, pp. 247–249.

[6] D. Lanaia and M. Marchetto, "ISAC-II Phasing High Level Appliacation in MATLAB", TRIUMF, Tech. Rep. TRI-DN-13-18, 2014.

[7] R. Baartman, "TRANSOPTR: Changes since 1984", TRIUMF, Tech. Rep. TRI-BN-16-06, 2016.

[8] R. A. Baartman, "Fast Envelope Tracking for Space Charge Dominated Injectors", in *Proc. 28th Linear Accelerator Conf. (LINAC'16)*, East Lansing, MI, USA, Sep. 2016, pp. 1017–1021. doi:10.18429/JACoW-LINAC2016-FR1A01